8.2 A 260GHz Broadband Source with 1.1mW Continuous-Wave Radiated Power and EIRP of 15.7dBm in 65nm CMOS

Ruonan Han, Ehsan Afshari

Cornell University, Ithaca, NY

Terahertz spectroscopy using silicon technology is gaining attraction for future portable and affordable material identification equipment. To do this, a broadband THz radiation source is critical. Unfortunately, the bandwidth of the prior CMOS works is not sufficient. In [1], the 300GHz signal source achieves 4.5% tuning range by changing the coupling among multiple oscillators. In [2], the DAR array has 3% tuning range with radiation capability. Alternative to the continuous device-tuning method, THz time-domain spectroscopy utilizing the broadband spectrum of picosecond pulses is widely used in the optics community [3]. In this paper, a high-power pulse-based sub-millimeter-Wave radiation source using 65nm bulk CMOS technology is reported. The architecture of this transmitter is shown in Fig. 8.2.1, where four differential core oscillator pairs are mutually coupled through four quadrature oscillators. Each core oscillator pair generates 2nd-harmonic signals at 260GHz that are power-combined after radiating through eight on-chip antennas. Four shunt switches, controlled by narrow pulses (width≈45ps) modulate the radiation. The pulses are generated by local digital circuit blocks with programmable repetition rate up to 5GHz. This way, the broadband spectrum of the pulses is upconverted to the carrier frequency of 260GHz. Without modulation, the chip achieves a continuous-wave radiated power of 1.1mW. Under modulation, the measured bandwidth of the source is 24.7GHz, which makes it suitable for many FTIR-based THz spectrometers. In addition, if the switches are modulated by digital data, this chip can also be used as a transmitter for sub-millimeter/THz wireless communications.

Due to the large attenuation and low detection sensitivity in this frequency range, high-power generation from the core oscillators is critical. It is demonstrated in [4] that the generated power in a transistor is mainly determined by the voltage phase shift, φ_A, between its gate and drain terminals. Moreover, the optimum phase shift value decreases from 180° when the fundamental oscillation frequency is over 100GHz. To achieve such phase shift, a three-stage topology with 3rd-harmonic extraction is proposed in [4]. However, a differential structure with 2nd-harmonic extraction is more desirable for the integration of large-sized on-chip antennas and symmetrical coupling with adjacent oscillators for power combining. Extracted power from a lower harmonic number is also higher. Unfortunately, the push-push topology used in previous works has a φ_A of 180° or higher, which leads to low fundamental oscillation and harmonic generation power. To solve this issue, we propose to use a transmission line as the feedback path across each transistor, plus two reactive components Y_1 and Y_2 at the gate and drain, to excite oscillation (Fig. 8.2.2). To determine the optimum impedance Z_0 and phase shift (length) φ_{TL} of the line, the Y-parameters of the entire network, $[Y_{total}]$, are derived. When oscillation occurs, the net currents I_1 and I_2 flowing into this self-sustained network are zero. Such analysis then provides the value of Z_0 and φ_{TL} needed to achieve a certain value of φ_A in the equation listed in Fig. 8.2.2. Figure 8.2.2 also shows the simulated output power as a function of φ_A and corresponding φ_{TL} and Z_0 for a 65nm CMOS transistor (W/L=27μm/60nm) at 130GHz. It can be seen that the optimum φ_A of 150° results in 2× larger power compared with a conventional push-push topology (φ_A=180°).

Next, a differential oscillator is formed by combining two of these units using coupled transmission lines (Fig. 8.2.2). Due to symmetry, two coupling modes can exist: in-phase and out-of-phase oscillations. The characteristic impedance of the coupled lines at these two modes is Z_{odd} and Z_{even}, respectively. The out-of-phase oscillation mode is desirable since it facilitates the extraction of the 2nd harmonic, and makes the Q of the coupled transmission line higher due to the constructive superposition of the magnetic field. By selecting φ_{TL} of 48° and Z_{even} of 60Ω, the generated power in out-of-phase mode is maximized as shown in Fig. 8.2.2. At the same time, Z_{odd} is designed to be around 20Ω which results in much lower generated power in the in-phase mode that is suppressed by the circuit loss. Finally, in conventional push-push and triple-push oscillators, the generated harmonics at the drain are greatly attenuated by the gate of the other transistor as it is directly connected to the drain. In our proposed structure, the line with $2\varphi_{TL}$ phase shift at $_0$ isolates the drain of each transistor from the gate, by transforming C_{gs} into a larger impedance as shown in the Smith Chart of Fig. 8.2.2. This means most of the generated power at $_0$ flows into the output through TL_2.

Other circuit blocks are presented in Fig. 8.2.3. To facilitate the placement of the antennas and the low-loss THz switching, each core oscillator pair should have out-of-phase 2nd-harmonic generation, thus 90° phase shift at the fundamental. So the core oscillators are mutually coupled by four quadrature oscillators. The quadrature oscillator is a ring of four identical amplifier stages with 270° phase shift and end-to-end simultaneous conjugate matching [5]. The differential switches use tuned MOS varactors (12fF), which have an ON/OFF impedance ratio of 21× at 260GHz compared to the 4× of PMOS. To accommodate the broadband radiation, slot antennas are used. Without having a ground reflector, the formed low-Q resonance cavity enables ~60GHz impedance matching ($|S_{11}|$<-10dB). The wide metal plane for current conduction in the slot antenna reduces loss. Additionally, not requiring large empty space for radiation, the slots can be closely placed into the transmitter layout for a compact, efficient feed-line network. Finally, a high-resistivity hemispheric silicon lens (diameter=10mm) is attached to the chip backside to eliminate the substrate-wave excitation. The beams are power-combined inside the lens, and the simulated radiation efficiency is 60%.

The testing setup is shown in Fig. 8.2.4. The chip is measured by a diagonal horn antenna cascaded by a VDI WR-3.4 even harmonic mixer (EHM) using the 16th harmonic of the LO. The oscillation frequency is measured to be 260GHz and the IF spectrum is shown in Fig. 8.2.5. The frequency can be continuously tuned within a range of 3.7GHz using the varactors in the core oscillators. The measured phase noise is -78.3dBc/Hz at 1MHz offset. The chip radiation patterns in E-plane and H-plane are also characterized (Fig. 8.2.5), resulting in a measured directivity of 15.2dBi. When using pulse modulation with a 3.5GHz repetition rate, the radiation spectrum is measured by sweeping the mixer LO, and is plotted in Fig. 8.2.6. The spurs above the equipment noise floor demonstrate a bandwidth of 21GHz. Since this spectrum can be continuously shifted by 3.7GHz, the radiation covers the entire 24.7GHz bandwidth. The actual output bandwidth predicted by the simulated radiation spectrum in Fig. 8.2.6 is over 40GHz. Finally, at a distance of 4.5cm from the chip, the measured continuous-wave power using the direct-detection mode of the mixer (responsivity=3kV/W) is 48μW, which is also verified with an Erikson PM4 calorimeter. This gives 15.7dBm EIRP and 1.1mW total radiated power. The chip consumes 0.8W power from a 1.2V supply. A die micrograph and performance comparison with prior work are given in Fig. 8.2.6. This source demonstrates the highest radiated power, EIRP, and bandwidth among all CMOS implementations in the table.

Acknowledgements:
The authors acknowledge the TSMC University Shuttle Program for chip fabrication, and the support of the C2S2 Focus Center under the FCRP, an SRC entity, and the National Science Foundation.

References:
[1] Y. Tousi and E. Afshari, "A 283-to-296GHz VCO with 0.76mW Peak Output Power in 65nm CMOS," *ISSCC Dig. Tech. Papers*, pp. 258-260, Feb. 2012.
[2] K. Sengupta and A. Hajimiri, "A 0.28THz 4×4 Power-Generation and Beam-Steering Array," *ISSCC Dig. Tech. Papers*, pp. 256-257, Feb. 2012.
[3] H. Liu, H. Zhong, N. Karpowicz, Y. Chen and X. Zhang, "Terahertz Spectroscopy and Imaging for Defense and Security Applications", *Proc. of IEEE*, vol. 95, no. 8, pp. 1514-1527, Aug. 2007.
[4] O. Momeni and E. Afshari, "High Power Terahertz and Sub-Millimeter-Wave Oscillator Design: a Systematic Approach," *IEEE J. Solid-State Circuits*, vol. 46, no. 12, pp. 583- 597, Dec. 2011.
[5] L. Franca-Neto, R. Bishop and B. Bloechel, "64GHz and 100GHz VCOs in 90nm CMOS Using Optimum Pumping Method," *ISSCC Dig. Tech. Papers*, pp. 444-538, Feb. 2004.
[6] J. Park, S. Kang, S. Thyagarajan, E. Alon and A. Niknejad, "A 260 GHz Fully Integrated CMOS Transceiver for Wireless Chip-to-Chip Communication ," *IEEE Symp. VLSI Circuits*, pp. 48-49, June 2012.
[7] Y. Zhao, J. Grzyb and U. R. Pfeiffer, "A 288-GHz Lens-Integrated Balanced Triple-Push Source in a 65-nm CMOS Technology," *European Solid-State Circuits Conf.*, Bordeaux, France, pp. 289-292, Sept. 2012.

 978-1-4673-4516-3/13/$31.00

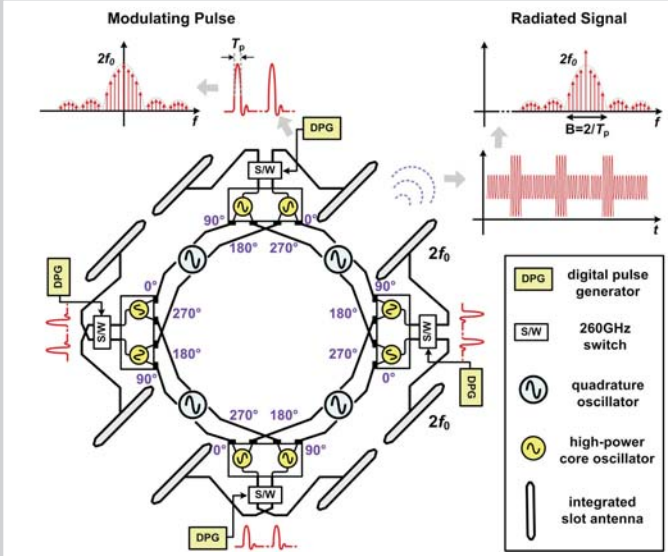

Figure 8.2.1: The architecture of the 260GHz broadband radiation source.

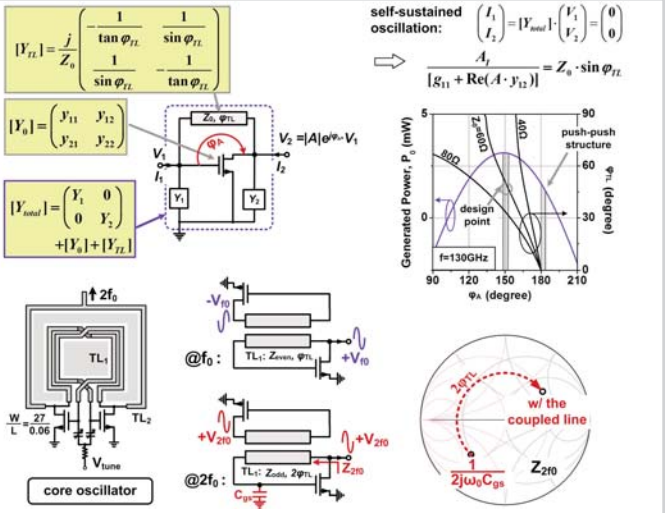

Figure 8.2.2: The design of the core oscillator. The structure simultaneously achieves the optimum phase and reduces the 2nd-harmonic loading from the gate.

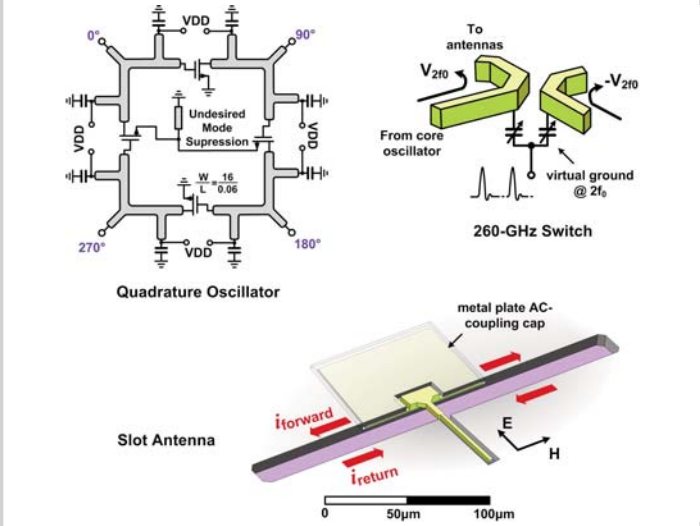

Figure 8.2.3: The designs of (top left) the quadrature oscillator, (top right) the varactor-based differential switch at 260GHz, and (bottom) the slot antenna.

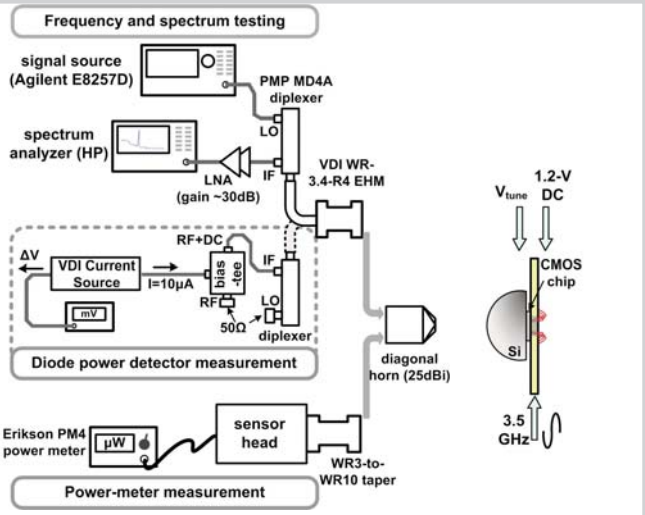

Figure 8.2.4: The setup for radiation frequency and spectrum measurement using harmonic mixer, and radiation power measurement using both diode power detector and calorimeter.

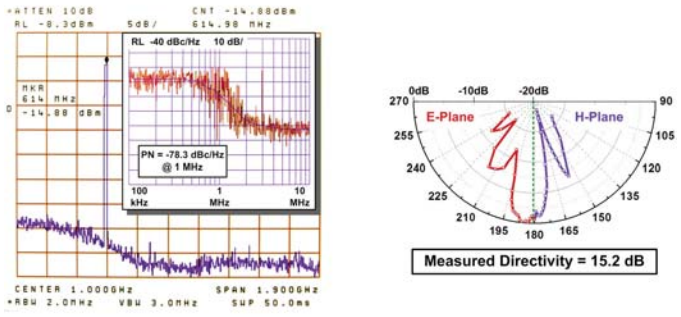

Figure 8.2.5: The measured IF spectrum, phase noise and the radiation pattern of the CMOS 260GHz source. Since the silicon lens is hemispheric, the radiated beam is not collimated by the lens.

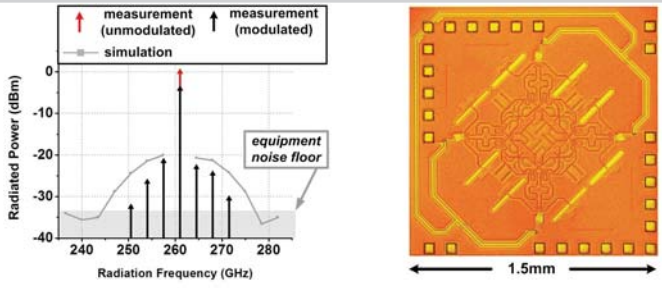

	ISSCC 2012 [1]	ISSCC 2012 [2]	VLSI 2012 [6]	ESSCIRC 2012 [7]	This Work
Frequency (GHz)	290	280	260	288	260
Bandwidth (%)	4.5	3.2	N/A	N/A	9.5
EIRP (dBm)	N/A	9.4	5	N/A	15.7
Output Power (dBm)	-1.2†	-7.2††	N/A	-4.1†††	0.5†††
Phase Noise	-78dBc/Hz @1MHz	N/A	N/A	-87dBc/Hz @1MHz	-78.3dBc/Hz @1MHz
DC Power (W)	0.32	0.81	0.69	0.28	0.8
Technology	65nm Bulk CMOS	45nm SOI CMOS	65nm Bulk CMOS	65nm Bulk CMOS	65nm Bulk CMOS

†: The output power is measured through probe landing, not radiation.
††: Wafer thinning to the silicon substrate is used.
†††: A silicon lens is used. The hemispheric lens shape in this work does not enhance the directivity.

Figure 8.2.6: The measured and simulated radiation spectrum, the chip die photo, and a table of performance comparison with the state-of-the-art sub-millimeter-wave signal sources.

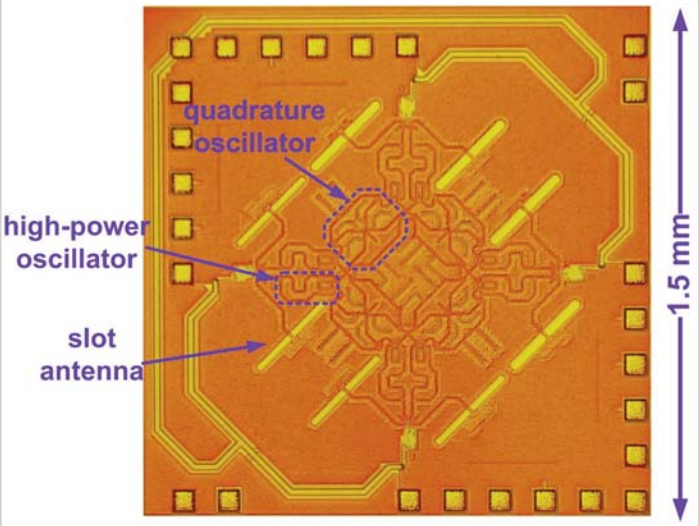

Figure 8.2.7: The die micrograph of the 260GHz radiation source

978-1-4673-4516-3/13/$31.00